COLLIDER ARCHITECTURE WORKING GROUP SUMMARY

Neville W. Reay
Ohio State University

Working Group Participants:

P. Avery (U. of Florida), R. Burnstein (Illinois Institute of Tech.),D. Christian (Fermilab), A. Clark (CERN), G. Coutrakon (Fermilab),J. Dorfan (SLAC), R. Edelstein (Carnegie-Mellon U.), K. Edwards (Carleton U., Canada), G. Feldman (SLAC), D. Hedin (Northern Illinois U.), P. Kenney (DOE), A. Kernan (U. of Cal. Riverside), R. Kephart (Fermilab), N. Lockyer (U. Penn.), K. McDonald (Princeton), D. MacFarlane (McGill), R. Morrison (U. of Cal. Santa Barbara), L. Roberts (Fermilab), R. Sidwell (Ohio State U.), J. Slaughter (Yale), D. Smith (U. of Cal. Riverside),N. Stanton (Ohio State U.), R. Stefanski (Fermilab), M. Witherell (U. of Cal. Santa Barbara).

Using the Fermilab collider as a Beauty factory opens formidable technical problems. The collider architecture working group attempted to consider the impact of the following challenges on the detector as a whole, using the previously submitted letters of intent[1] and the work done at the Berkeley SSC workshop[2] as starting points:

1) Triggering: What types of triggers appear promising?

2) Vertexing: Must part of the detector reside inside the beam pipe?

3) Detector Outer Geometry: Can there be a single type of magnetic field for the entire detector or are different magnetic geometries required for different angular regions?

4) Particle identification: What types of particle identification are needed and how do the requirements vary with production angle?

In light of the short time scale, many detailed questions were left for other appropriately charged groups. Further, as an in-depth development was not possible in a few days, we will simply point out areas in which a consensus was reached and others in which honest differences of opinion were not resolved.

The conceptual layout of the overall detector geometry, shown in Figure 1, was arrived at in the course of the discussions. Two possible inner tracking geometries are shown in Figure 2. How these layouts were chosen will become evident in the discussion which follows.

1. TRIGGERING

The theoretically expected ratio of the BBbar pair cross section to total inelastic cross-section is approximately $3x10^{-4}$, roughly a thousand times larger than the ratio for fixed-target experiments. Given the small branching ratios associated with rare decays and CP-violating effects, a useful trigger must access and tag a large percentage of the relevant beauty decays. ISAJET simulations by some of the participants prior to the workshop had indicated that a single-lepton trigger could access 5-10% of the signal with sufficient background rejection.

As these studies ignored possible misidentification of leptons in the trigger, considerable time was spent discussing this problem. Background rejection in excess of 10^4 per event means that lepton misidentification will have to kept below a $fewx10^{-4}$ per event. If this level is achieved, additional rejection could come from computationally intensive topological considerations such as requiring large impact parameters or rejecting kinked tracks resulting from charged pion or kaon decays.

An electron trigger in the central region appeared eminently feasible but very difficult. A PT cut of 1-2 GeV/c could be provided with minimal tracking plus electromagnetic calorimetry. Multi-stage transition-radiation detection (TRD) would be used to eliminate hadron misidentification, though severe constraints will be imposed by a lack of space.

More rejection per unit solid angle will be required in the forward-backward regions, as two thirds of all tracks and an equivalent number of photons are contained within cones of 20° half angle about the beam lines. A momentum cut of 5-10 GeV/c and a PT cut near 1.5 GeV/c will be required on the lepton in this region. A multi-stage tracking TRD also would be required to eliminate coalescing photon showers superimposed on hadron tracks.

Fast level II selection requiring some tracking also would be required. As shown in Figure 3, photons travel in straight lines prior to conversion, while electrons follow an arc in the magnetic field. By reconstructing this arc and checking the location of candidate electron showers most photon conversions downstream of the vertex detector could be eliminated. A comparison of candidate electron energy from pulse height and track momentum from bending in the magnetic field could further suppress misidentification of hadrons. Finally, an additional level III electron impact parameter selection could be made using vertexing information, but implementation of this is as yet an unsolved problem.

Turning now to muon tagging, UA1 experience indicated that muons with PT > 5 GeV/c could be selected easily, but that identifying muons with much less than 5 GeV total momentum was difficult. Because the Beauty mass scale is 5 GeV, imposing such a cut would eliminate most beauty events. Though liquid CRIDs were suggested as possible detection devices for central production, muon tagging appeared

an attractive option only in the forward-backward range of perhaps 50 to 400 milliradians where P is large. Muon steel would have to extend at least three meters along the beam lines in both directions and thus would determine the transverse scale of the experiment.

To minimize punch-through, which would be a severe problem at the smaller angles, frequent pulse-height sampling would be required inside the steel absorber. This sampling also could aid in selecting the upstream track corresponding to the muon. This latter connection would have to be made as part of the level II trigger, as half the pion decay and most of the kaon decay muons could be eliminated with track quality cuts in the high-resolution upstream system. A level III impact parameter cut would be required for muons as well as electrons, but how to do this is currently not understood.

Despite these reservations, everyone believed that muon detection was essential both for tagging and in the study of rare decays.

2. VERTEXING

The main impact of vertexing on architecture was the question of whether high-resolution elements were required inside the beam pipe. Detector outgassing, the need to retract detectors during filling, and extracting a half-million lines of information through vacuum walls would present serious difficulties for any experiment. However, if the vertexing system were placed outside the beam pipe, the distance and intervening multiple-scattering material could seriously degrade decay-vertex resolution. Discussions with DO, CDF and accelerator people opened the possibility of a beryllium beam pipe with less than one inch outer diameter and a wall thickness of 500 to 1000 microns. Multiple-scattering from such a device is shown in figure 4.

The uncertainty in impact parameter for a given track is given by

$$\delta X = L\left(\frac{0.022}{P}\sqrt{\left(\frac{X}{X_o \sin(\theta)}\right)}\right) = \frac{0.022\ R}{P_t}\sqrt{\left(\frac{X}{X_o \sin(\theta)}\right)}$$

$$\delta X = \frac{15\ \text{microns}}{P_t \sqrt{\sin(\theta)}}$$

It appears possible to maintain a resolution of better than 30 microns for most tracks with vertex devices mounted external to the beam pipe, though annular rings spaced at wide intervals inside the beam pipe might be advantageous for forward-backward tracks. This, if true, greatly simplifies the Beauty collider experiment.

A second point about vertexing is that for angles near the beam lines it is possible to implement a silicon microstrip vertex system with the 12-18 track samples minimally needed to construct track vectors and perform pattern recognition. For the bulk of the 4π solid angle at most four samples are possible. To lowest order, this

means that the silicon delivers only a single point with 5-10 micron accuracy while pattern recognition falls onto gas detectors, which must furnish 50-100 points with resolution ranging from 25-50 microns near the silicon up to 100-150 microns at larger radii. They also must have good two-track separation and furnish three views with full accuracy in (r,θ,ϕ). Further, the local geometry of the gas detector must be engineered to permit quick on-line extrapolation into the silicon.

The gas detector therefore becomes a hybrid whose inner geometry is driven by the vertexing system while its outer geometry is dictated by the topology of the magnetic field.

3. DETECTOR OUTER GEOMETRY

Early in the workshop it became clear that the topology of the magnetic field required for momentum analysis of charged tracks would have a decisive impact on the outer topology of the detector. All ISAJET studies of beauty decay tracks had momentum versus angle distributions as shown in Figure 5. Forward-backward tracks have momenta in the tens of GeV/c range while the bulk of tracks in the central region lie below 5 GeV/c. A typical beauty event is shown in Figure 6.

Note that the beauty decay tracks are scattered throughout the detector. The magnetic field integral therefore must be greater for tracks along than for tracks perpendicular to the beam line and must vary smoothly over 4π solid angle. After a great deal of discussion, a consensus formed that the geometry of choice was a dipole field aligned perpendicularly to the beam lines. Forward-backward tracks would receive maximal field integral, while the field integral for central tracks would be decreased by the shorter distance of travel in the magnetic field and/or the smaller component of field perpendicular to the track, as shown in Figure 7. For most tracks the accuracy in $\delta P/P$ is dominated by multiple scattering.

Assume that a field of 1 Tesla extends 6 meters along the beam, half of which is useful for particles produced at the center of the detector. Assume one meter is available transverse to the beam for measuring bending in the magnetic field and that sagittas can be measured to an accuracy of 40 microns using multiple-sampling drift chambers. Finally, estimate a multiple scattering which varies from 4% of a radiation length in the forward direction down to 1% at 90°. The distance of travel perpendicular to the field needed to obtain $\delta P/P = 1\%$ and 3% under these assumptions for particles following the solid curve of Figure 5 is given in Figure 7.

Two magnetic-field geometries were considered; the UA1 style shown in Figure 2a and the cylindrical device with wires parallel to the magnetic field shown in Figure 2b.

The geometry of Figure 2a has the advantage of easy implementation of full stereo, so that decay vertices could be reconstructed in orthogonal views, but has the disadvantage of dead regions and perhaps large multiple scattering at the interfaces between detectors. The geometry of Figure 2b by taking full advantage of the symmetry

of the magnetic field has few dead regions, but precisely measures only one view. Despite considerable discussion, no single geometry was preferred by all participants.

4. PARTICLE IDENTIFICATION

As discussed in the triggering section, a great deal of attention was paid to identification of muons and electrons. ISAJET background studies indicated that if misidentification of hadrons as electrons and muons could be kept below a few x 10^{-4}, the background from this source to a single-lepton trigger would be acceptable. Presentations and information from other working groups indicated that these levels of rejection could be achieved for electrons with production angles larger than perhaps 50 milliradiams and muons with production angles between roughly 50 and 400 milliradians.

Some of the participants had studied hadron identification and believed π-K-p separation at the two standard-deviation level could be achieved for central tracks using 100 picosecond time-of-flight and liquid ring-imaging cerenkov counters with track depths as short as 20 cm. As shown in the layout of figure 2, 20 cm would present a problem only for tracks within a cone of perhaps 45° half angle about the magnetic field, for which detector thickness would reduce linearly the field integral available for momentum analysis.

Particle identification for tracks at small angles would require two-stage gas ring-imaging cerenkov counters occupying roughly 2 meters along the beam line on both sides of the central region, as shown in Figure 1. Such a length increases the probability for muon decay both of pions and kaons and almost doubles the transverse scale of the muon detector. Rejection power versus length, the segmentation required (particularly at small angles) and the balance between gas and liquid detectors required in-depth study beyond the scope of the workshop.

5. SUMMARY:

In summary, a single-electron trigger appears promising, but compromises somewhat the tracking volume in the central region. Single-muon identification without eliminating most of the beauty decays appears possible only in the forward-backward regions along the beam lines. Placing vertex detectors external to the vacuum pipe conceptually simplifies the detector and the magnetic geometry of choice is a dipole field transverse to the beam lines. Participants disagreed as to whether the gas-detector tracking geometry should eliminate dead spots by placing all sense-lines parallel to the magnetic field or concentrate more strongly on providing full two-view stereo. Particle identification appears possible over most of the solid angle, but may be limited to time-of-flight in the vicinity of the pole tips and conflicts with the desirability of a short drift space for decays in the forward-backward region.

The prospects for producing and detecting enough beauty to observe strong CP violation appear promising and exciting, but further study certainly is required.

REFERENCES

1. Fermilab Proposal 783: "Letter of Intent for a Tevetron Collider Beauty Factory". Fermilab Proposal 784: "Proposal for a Bottom Collider Detector".

2. Workshop on Experiments, Detectors and Experimental Areas for the Superconducting Super Collider, July 7-17, 1987, Berkeley, California

FIGURE CAPTIONS

Figure 1: Overall detector layout; for clarity the central tracking and particle identification have been omitted.

Figure 2: Geometry of inner tracking and particle-identification devices.
a) UA1-style tracking geometry in a dipole magnetic field. Refer to 2b for the geometry of particle identification apparatus.
b) Cylindrical gas tracking with wires arranged parallel to the direction of the dipole magnetic field.

Figure 3: Sketch indicating that photons converting after passing through a magnetic field would have a large impact parameter if assumed to be electrons coming from a Beauty decay.

Figure 4: Schematic of multiple scattering in the beam pipe.

Figure 5: Scatter plot for momentum versus angle distribution for charged decay tracks from Beauty decays. The solid curve is used as input for the momentum resolution versus production angle curves exhibited in Figure 7.

Figure 6: IASJET-generated beauty decay; all tracks shown are from beauty decays.

Figure 7: Polar plot showing field integral versus production angle θ. Curves (a), (b), (c) and (d) have been generated for ϕ azimuthal angles of 0°,45°,60° and 90°. When $\phi = 0^o$, particles are produced in a plane perpendicular to the magnetic field. The $\delta P/P$ = 1% and 3% curves indicate the minimum length of travel perpendicular to a 1 Tesla magnetic field required to obtain the stated resolution for particles having the dependence of momentum on angle given by the solid curve of Figure 5. A total error of 40 microns is assumed for sagittas determined by multiple-sampling drift chambers and multiple scattering is assumed to vary from 1% near $\theta = 90^o$ up to 4% near zero degree production.

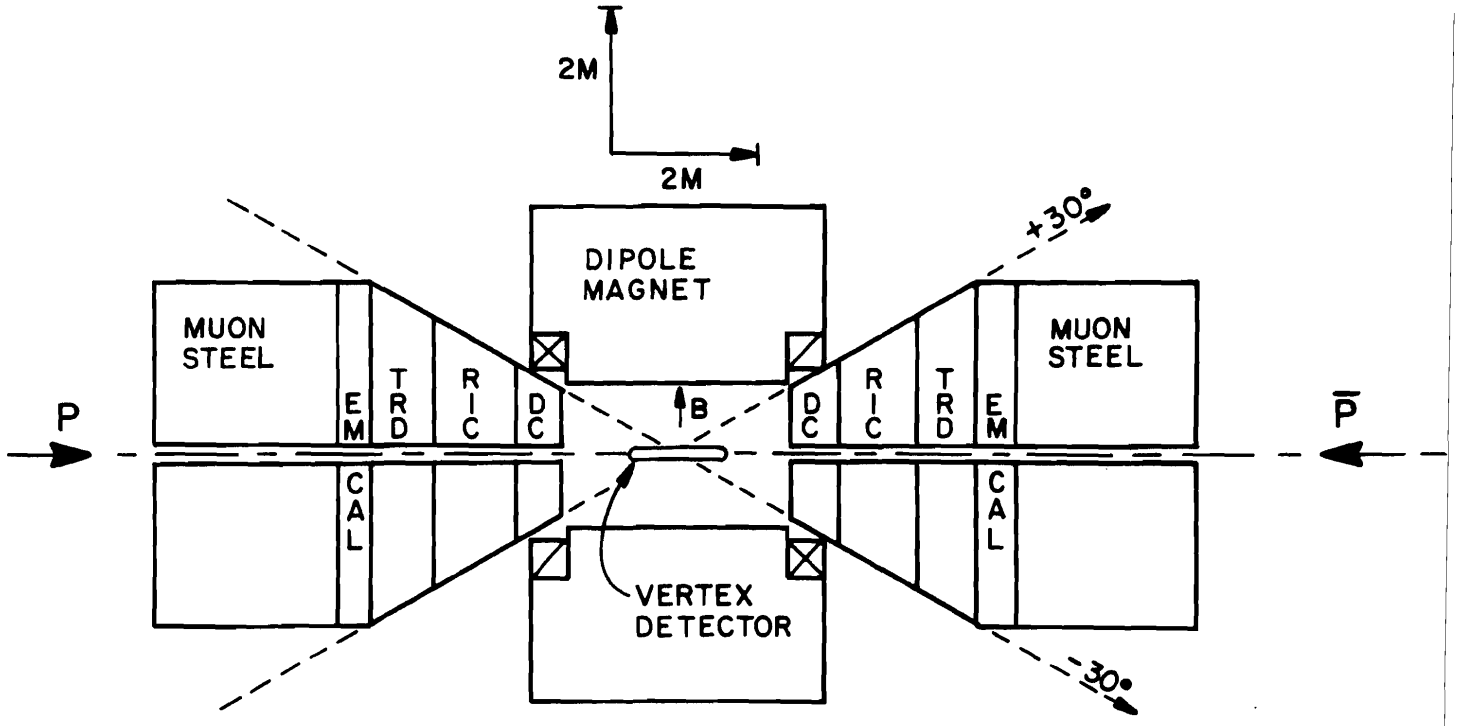

Figure 1

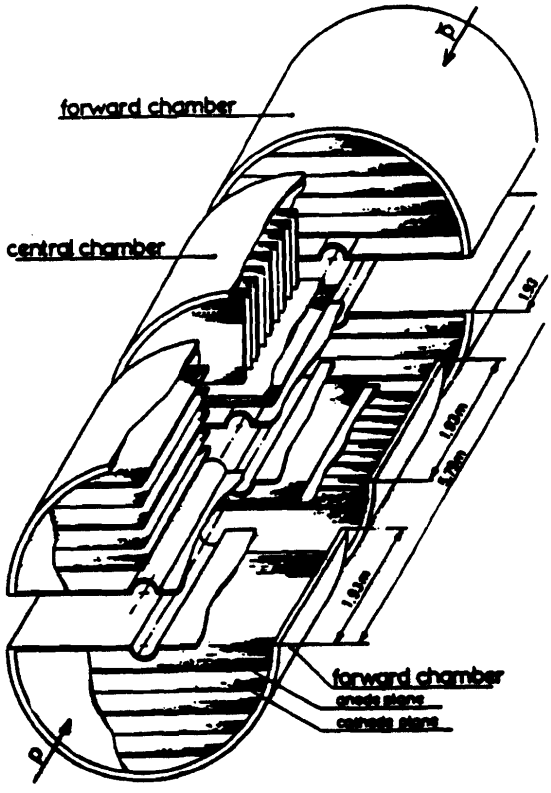

Figure 2a

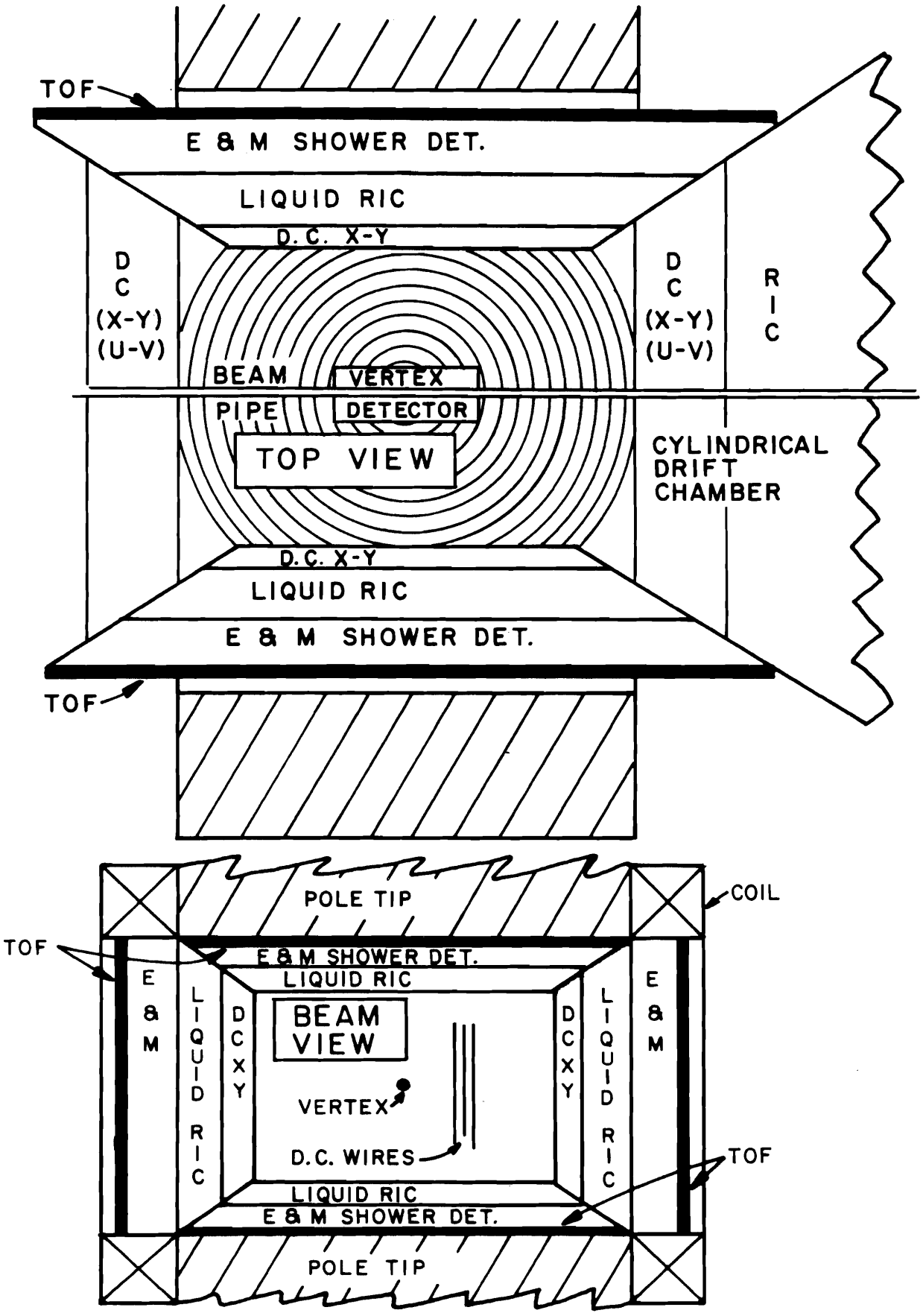
TOF
E & M SHOWER DET.
LIQUID RIC
D.C. X-Y
D C (X-Y) (U-V)
D C (X-Y) (U-V)
R I C
BEAM PIPE
VERTEX DETECTOR
TOP VIEW
CYLINDRICAL DRIFT CHAMBER
D.C. X-Y
LIQUID RIC
E & M SHOWER DET.
TOF
POLE TIP
COIL
TOF
E & M SHOWER DET.
LIQUID RIC
E & M
LIQUID RIC
DCXY
BEAM VIEW
VERTEX
D.C. WIRES
DCXY
LIQUID RIC
E & M
TOF
LIQUID RIC
E & M SHOWER DET.
POLE TIP

Figure 2b

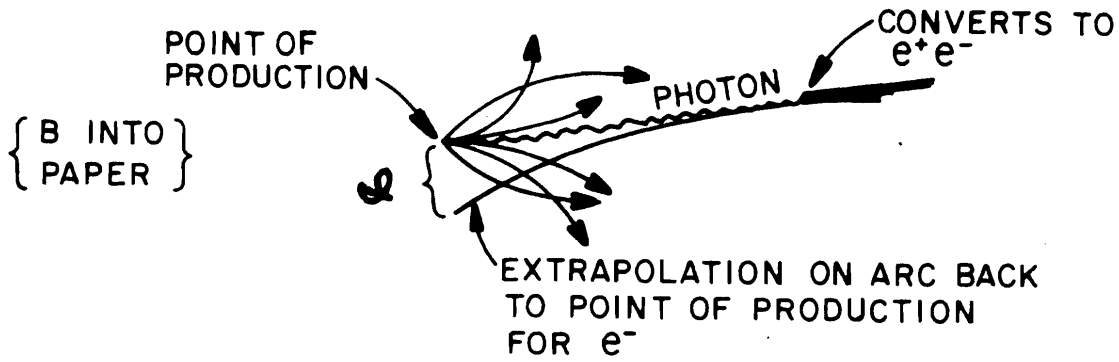

Figure 3

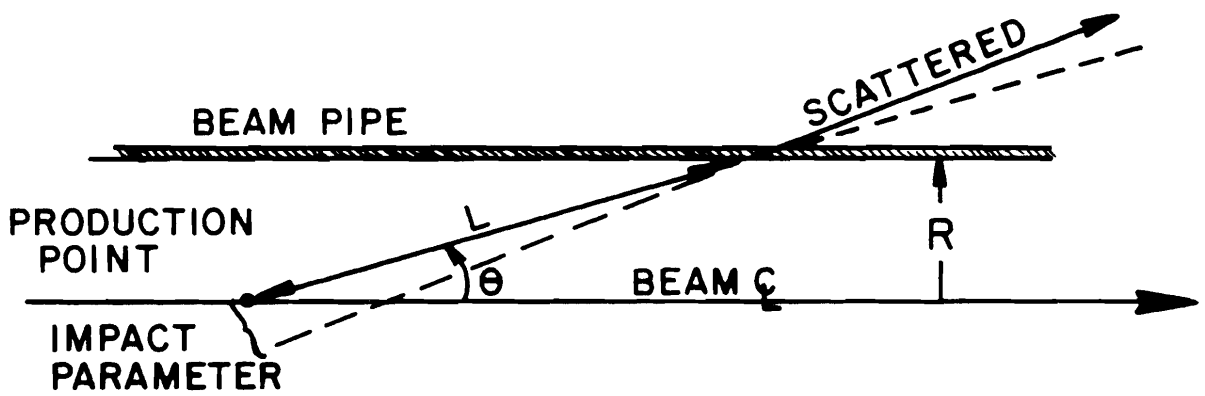

Figure 4

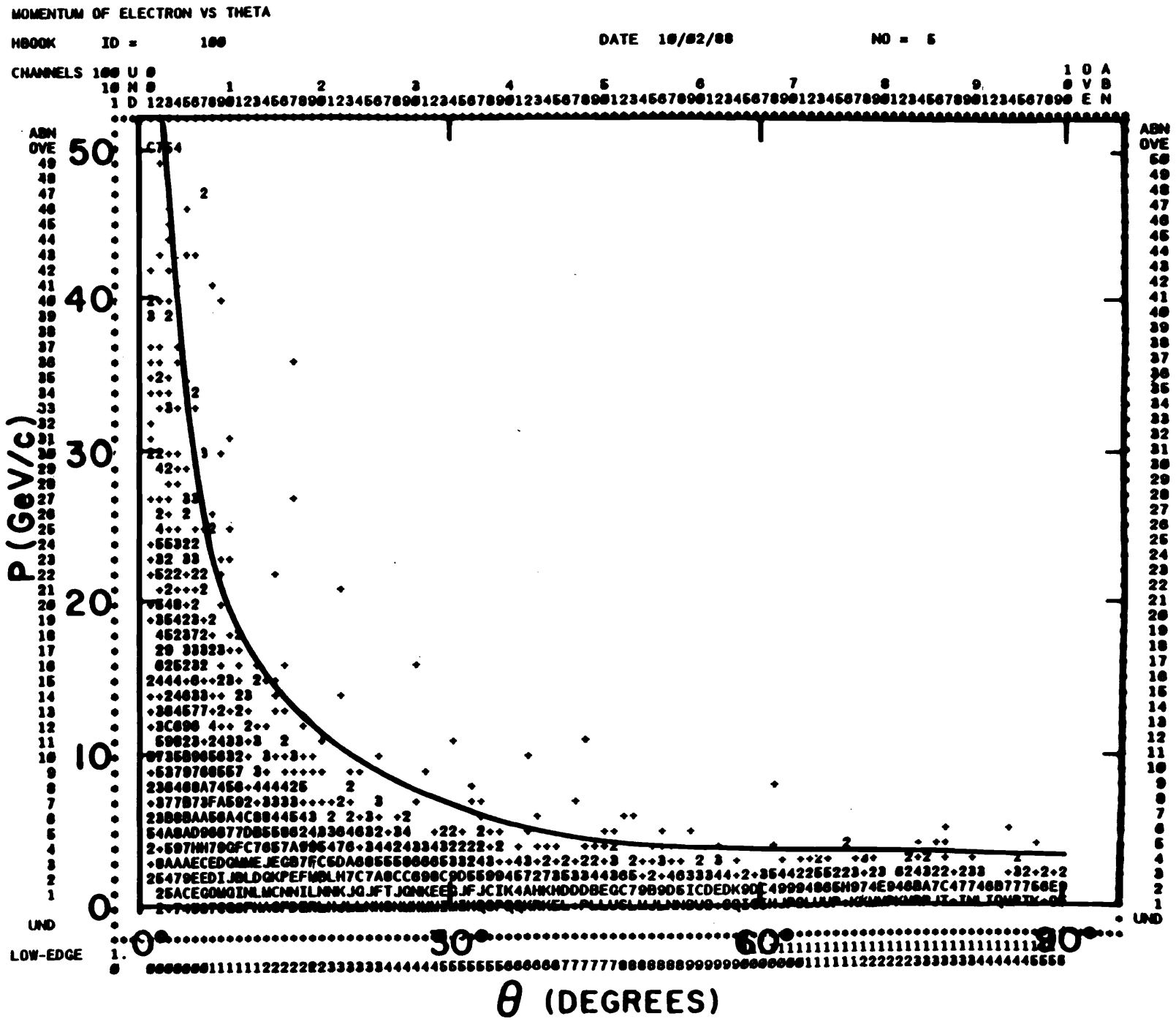
MOMENTUM OF ELECTRON VS THETA
HBOOK ID = 100
DATE 10/02/88
NO = 5
CHANNELS 100
P (GeV/c)
θ (DEGREES)
LOW-EDGE
UND
OVE
ABN

Figure 5

B_u^- (P_L = 2.7, P_T = 4.3 GeV)

↳ $D^0 + 2\pi^+ + 3\pi^- + 2\pi^0$

↳ $K^-\pi^+\pi^0$

$\overline{B}_u^+$ (P_L = 17, P_T = 1.7 GeV)

↳ $D^- + 2\pi^+ + 2\pi^0$

↳ $K^+\pi^-\pi^-\pi^0$

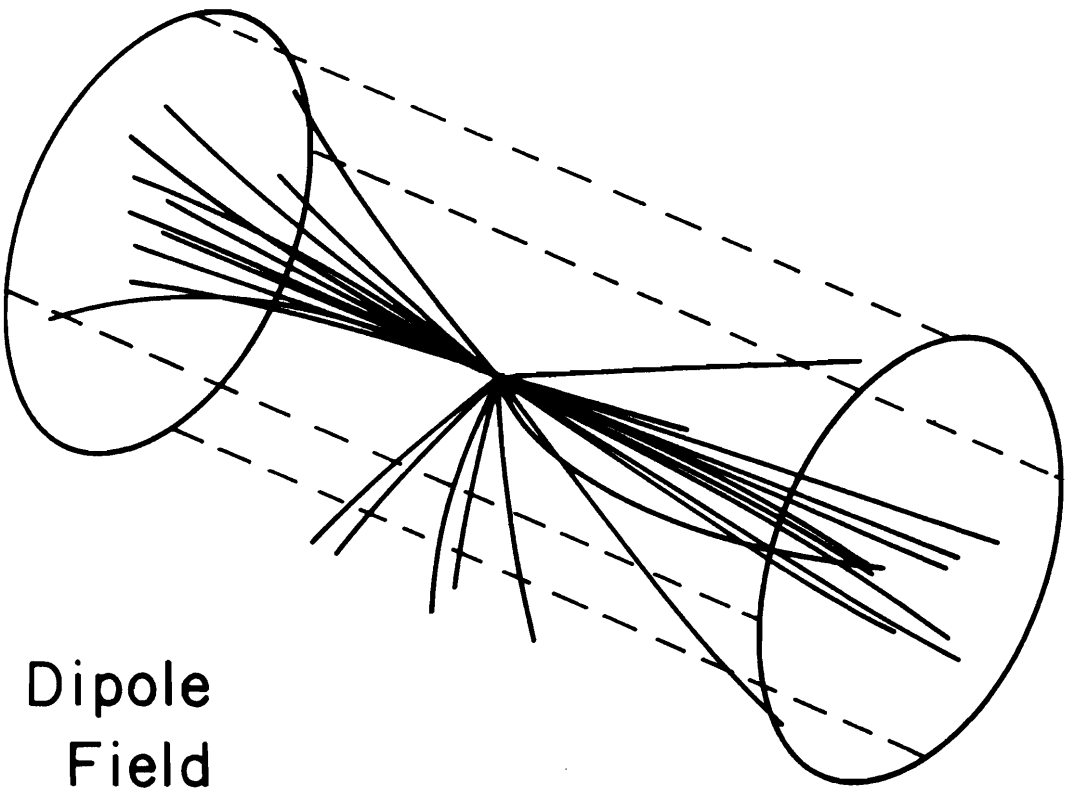

L. Roberts

Figure 6

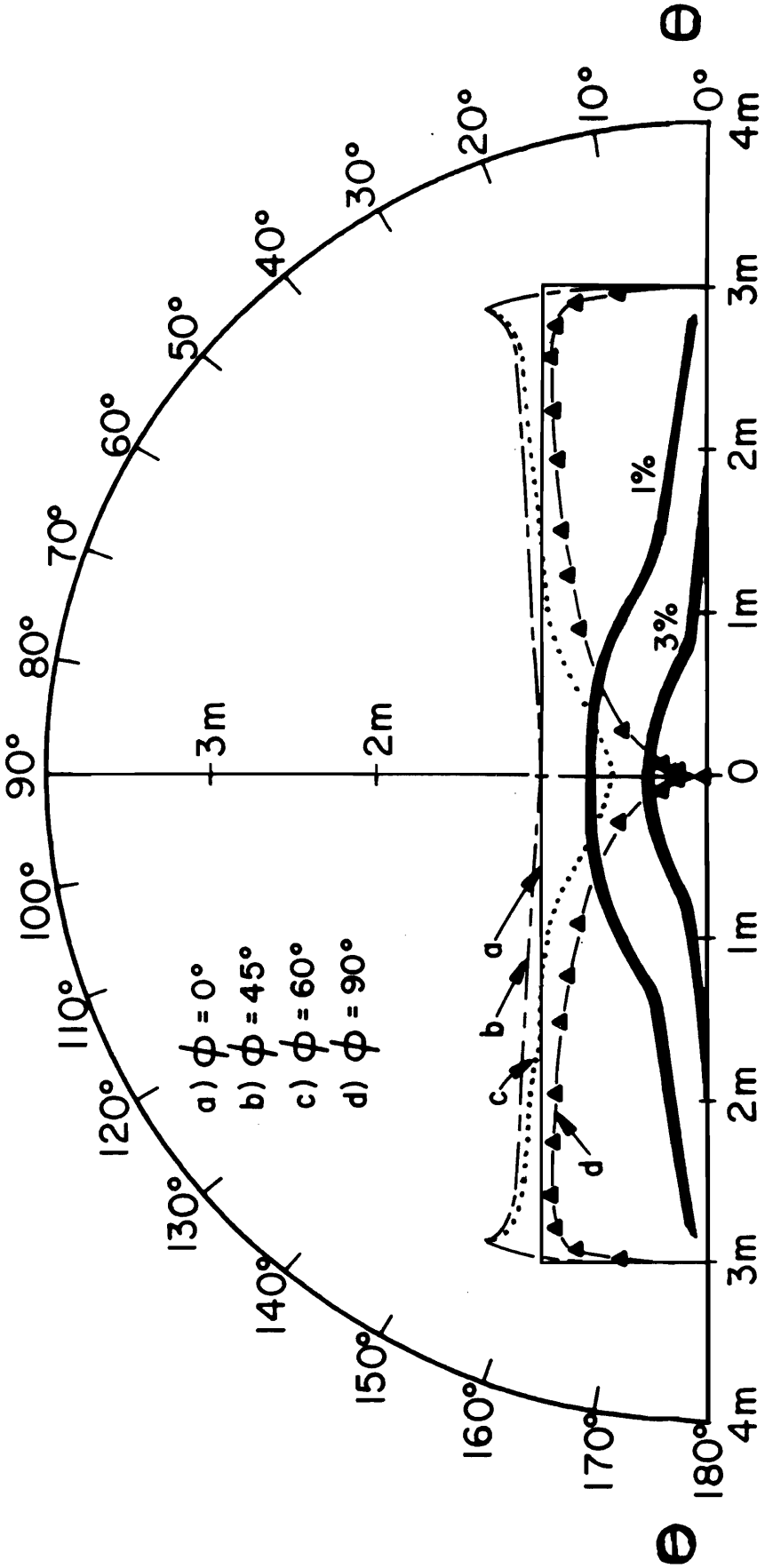
θ
0°
10°
20°
30°
40°
50°
60°
70°
80°
90°
100°
110°
120°
130°
140°
150°
160°
170°
180°
4m
3m
2m
1m
0
1m
2m
3m
4m
1%
3%
a
b
c
d
a) φ = 0°
b) φ = 45°
c) φ = 60°
d) φ = 90°
θ

Figure 7